Effect of Ions on a Dipalmitoyl Phosphatidylcholine Bilayer. A Molecular Dynamics Simulation Study

Arnau Cordomí,[†] Olle Edholm,[‡] and Juan J. Perez*,[†]

Department of Chemical Engineering, Technical University of Catalonia (UPC), Av. Diagonal 647, 08028 Barcelona, Spain, and Theoretical Biological Physics, Royal Institute of Technology (KTH), SE-10691 Stockholm, Sweden

Received: May 20, 2007; In Final Form: October 26, 2007

The effect of physiological concentrations of different chlorides on the structure of a dipalmitoyl phosphatidylcholine (DPPC) bilayer has been investigated through atomistic molecular dynamics simulations. These calculations provide support to the concept that Li^+, Na^+, Ca^{2+}, Mg^{2+}, Sr^{2+}, Ba^{2+}, and Ac^{3+}, but not K^+, bind to the lipid-head oxygens. Ion binding exhibits an influence on lipid order, area per lipid, orientation of the lipid head dipole, the charge distribution in the system, and therefore the electrostatic potential across the head-group region of the bilayer. These structural effects are sensitive to the specific characteristics of each cation, i.e., radius, charge, and coordination properties. These results provide evidence aimed at shedding some light into the apparent contradictions among different studies reported recently regarding the ordering effect of ions on zwitterionic phosphatidylcholine lipid bilayers.

Introduction

Biological membranes are not only essential for cell integrity, providing a barrier between the interior and the exterior of a cell, but also as a matrix and support for many types of proteins involved in important cell functions. Moreover, growing experimental evidence regarding the importance of the lipid membrane on protein function has recently attracted the interest of the scientific community.[1] However, the current knowledge about biological membranes is still scarce, due to the difficulties associated to the experimental techniques required. The present view of the membrane is based on the fluid mosaic model[2] where proteins are distributed in regions of biased composition with varying protein environment.

Atomistic molecular dynamics (MD) simulations of lipid bilayers provide a detailed microscopic picture of the interactions and processes in biological membranes that are not accessible by experimental methods. Still, the complexity of real membranes, containing many different proteins, lipids, and other molecules, are not affordable presently for atomic scale modeling. For this reason, the study of model one-component model lipid bilayers have been the focus of attention of a large number of reports published in recent years, which have been pivotal in order to provide new insights into this subject.[3−9] The increasing computer power in recent years has offered the possibility to study more complicated systems such as phospholipid mixtures[10−12] and/or the inclusion of other compounds such as cholesterol[13−15] or ions.[16−22]

Since membranes at physiological conditions are in contact with electrolyte solutions, their specific interactions with ions are a matter of substantial interest.[23] Experiments performed in the last few decades show that ions play an essential role not only in the structure, dynamics, and stability of membranes but also for the binding and insertion of proteins, membrane fusion, and transport across membranes.[24−35] The specific binding of ions to lipid bilayers has been studied in a variety of systems including both negatively charged and zwitterionic lipids. For charged lipids, the obvious role of ions is to compensate for the lipid charge.[36,37] However, several studies have confirmed that ions interact in an analogous way as in zwitterionic lipid bilayers.[18−22]

Despite experimental evidence that ions may alter the structural properties of lipid bilayers,[38,39] the difficulties associated with precise experimental determinations still leave questions open. Thus, in a recent study of ion binding to a phosphatidylcholine (PC) bilayer the authors showed that certain ions, including different divalent ones and Li^+, affect the gel to liquid-crystal transition.[40] In recent heat capacity measurements, the authors provided evidence that Na^+ reduces the area per lipid in bilayers of zwitterionic PC bilayers.[21] Similarly, in a recent study, the differences observed in the nanomechanical properties of lipid bilayers with different electrolytes could only be explained as due to the increased lipid ordering originated by ion binding.[41] Finally, in a recent X-ray diffraction study it was found that K^+ ions do not alter the structure of PC bilayers,[42] showing an apparent differential behavior of potassium.

MD simulations of lipid bilayers with ionic solutions show that ions reduce the area per lipid for negatively charged lipids[16,17,37,43] as well as for zwitterionic ones.[18,21,22] Moreover, in a very recent MD study on ion penetration into PC bilayers almost no stable binding of K^+ ions to the lipid groups was observed, although the use of various force-fields yields different results.[44] The aim of this work is to understand the effect of different ions on the properties of the lipidic membrane and to analyze the differential behavior due to charge and size. For this purpose, eight 40 ns MD simulations of DPPC bilayers have been performed with a 0.2 M concentration of XCl_N, where X = Li^+, Na^+, K^+, Mg^{2+}, Ca^{2+}, Sr^{2+}, Ba^{2+}, and Ac^{3+}, and N is the cation charge. Despite the lack of biological interest in lithium, strontium, barium, and actinium, they were included to cover a larger range of ion parameters. Additionally, the effect

[†] Technical University of Catalonia (UPC).
[‡] Royal Institute of Technology (KTH).

10.1021/jp073897w CCC: $40.75 © 2008 American Chemical Society
Published on Web 01/15/2008

of electrolyte concentration was tested by performing simulations with NaCl and KCl at 1 M concentration. The effects of the different ions were compared with a simulation of a pure DPPC bilayer in water that was used as reference. Present results indicate that ions Li^+, Na^+, Mg^{2+}, Ca^{2+}, Sr^{2+}, Ba^{2+}, and Ac^{3+} bind to the head-groups of DPPC and alter structural properties of the bilayer such as the area per lipid or the lipid head dipole orientation. However, potassium ions behave in a different manner, not binding to the head-groups and leaving the properties of the bilayer close to those of a bilayer in pure water. These results are consistent with all the experimental evidence available in the literature. However, because of the different results for potassium obtained in previous MD simulations, attributable to the force-field,[44] it cannot be excluded that, using a different force-field or longer simulation times, ions could penetrate the head-group without affecting structure and area per lipid of the bilayer. Further investigation of the effects of ion parameters to be used in simulations with lipid bilayers is needed.

Methods

Molecular Dynamics Simulations. All computer simulations were performed using the parallel version of the GROMACS 3.2 package.[45,46] Each system was subject to periodic boundary conditions in the three coordinate directions. The temperature was kept constant at 323 K (well above the gel/liquid crystalline phase transition temperature of 314 K) using separate thermostats for lipids, water, and ions.[47] The time constant for the thermostats was set to 0.1 ps except for water, for which a smaller value of 0.01 ps was used. The pressure was kept at 0.1 MPa in the three coordinate directions using independent Berendsen barostats with a time constant of 1.0 ps.[47] A flexible cell geometry was chosen with the use of the NPT ensemble since other commonly used ones such as the NVT or the NP_z-AT inherently fix the area per lipid.[19,48,49] The equations of motion were integrated using the leapfrog algorithm with a time step of 4 fs. All bonds were kept frozen using the LINCS algorithm.[50] The bonds and the angle of the water molecules were fixed using the analytical SETTLE method. Lennard−Jones (LJ) interactions were computed with a cutoff of 1.0 nm, and the electrostatic interactions were treated with the Particle Mesh Ewald (PME) procedure.[51] DPPC lipids were modeled using a variation of the force-field parameters described in ref 4, in which LJ parameters are computed as combinations of the single atomic ones according to the combinations rules of the OPLS-AA implementation in GROMACS. These parameters have been used in recent simulations of rhodopsin embedded in DPPC bilayers[52] and equally reproduce the experimental area per lipid of pure DPPC bilayers in the liquid crystalline phase.[4,13,53] Finally, ion parameters (listed in Table 1) were taken from the OPLS-AA force-field[54] currently implemented in GROMACS, and water molecules were treated using the TIP3P model.[55] Although different ion force-fields provide different results in specific properties,[56] the choice of the ion parameters does not appear to be critical for the purpose of the present work. Specifically, we computed the interaction energy between the different cation−oxygen pairs in the present work (data not shown), concluding that, first, differences in the cation−oxygen interactions for any oxygen type in the most commonly used force-fields are small, and second, the preceding differences for a specific cation are smaller than those between different cations. This suggests that cation−oxygen interaction energies follow the same trend independently of the parameters chosen even if combining different force-fields.

TABLE 1: Cationic Properties in the Present Study

ion	$*\sigma$ (nm)[a]	$*\epsilon$ (kJ/mol)[a]	rdf cutoff (nm)[b]	est. radii (nm)[c]
Li^+	0.2126	0.0765	0.27	0.071
Na^+	0.3330	0.0116	0.31	0.103
K^+	0.4935	0.0014	0.36	0.143
Mg^{2+}	0.1644	3.6636	0.24	0.070
Ca^{2+}	0.2412	1.8826	0.30	0.103
Sr^{2+}	0.3103	4.9499	0.34	0.119
Ba^{2+}	0.3817	0.1972	0.33	0.141
Ac^{3+}	0.3473	0.2261	0.33	0.119

[a] OPLS Lennard−Jones parameters with Gromacs version 3.2 used for the cations (file ffoplsaanb.itp). [b] Largest cation−oxygen distance for a water molecule in the first coordination shell taken from oxygen/cation RDF. [c] Estimate of the ionic radii is given as the position of the first peak of the oxygen/cation rdf less 0.137 nm (see text).

Starting Simulation Boxes. Binding of cations to a PC bilayer, starting from a random distribution of cations in the solvent, requires long simulation times since ions have to reach the water/lipid interphase region, a process that occurs in several tens of nanoseconds for some ions.[22] With the aim of saving computer time, the starting boxes for the different simulations of the present work were generated from a previous simulation of a pure DPPC bilayer with water and sodium chloride.[52] This system contained 256 lipids, ∼17 000 water molecules, corresponding to a hydration of 66 waters per lipid, and 61 sodium and 61 chloride ions, giving a concentration of sodium chloride of about 0.2 M. This box was generated in a simulation where electrostatic interactions were treated by using a twin cutoff of 1.0/1.8 nm and charge groups distributed in a way known to give artificially small areas in bilayers without ions.[53,57,58] This procedure allows measurement of steady values for the area per lipid in less than 25 ns since the binding of cations to the lipid head-groups also reduces the area per lipid. This idea is supported by the fact that when ions are placed using a potential-based function, steady values of the area per lipid are obtained much faster than when using a random placing.[59] The initial size of the simulation boxes was $8.1 \times 8.1 \times 12.7$ nm^3 (XYZ), the first two dimensions being those of the bilayer plane which corresponds to an area of 0.51 nm^2 per lipid.

Starting from the DPPC box containing 0.2 M NaCl, the remaining boxes with the same ion concentration were generated by replacing the sodium ions with the other cations. Moreover, the starting system containing NaCl is not in equilibrium when performing the simulations using the PME method. In the systems with divalent and trivalent ions, 61 or 122 water molecules were replaced by chloride ions to obtain an electroneutral system. In the case of the simulations of NaCl and KCl at 1 M, 486 additional water molecules were substituted by 243 sodium and 243 chloride ions. In both cases, the ions were located at the most electrostatically favorable positions, using the GENION program from the GROMACS toolbox.

Results and Discussion

The present simulations show that with the exception of KCl, the rest of the systems exhibit the ions distributed in a double layer where the cations are closer to the bilayer than the chloride ions, generating a dipole in opposition to the one produced by the lipid head-groups. Moreover, cations are actually bound to the carbonyl or to the phosphate oxygens of the polar head-groups, whereas ions not bound are uniformly distributed in the water phase. Ion binding to the lipid molecules has effects on lipid order and results in a different charge distribution compared to the system with no electrolyte. Systems containing

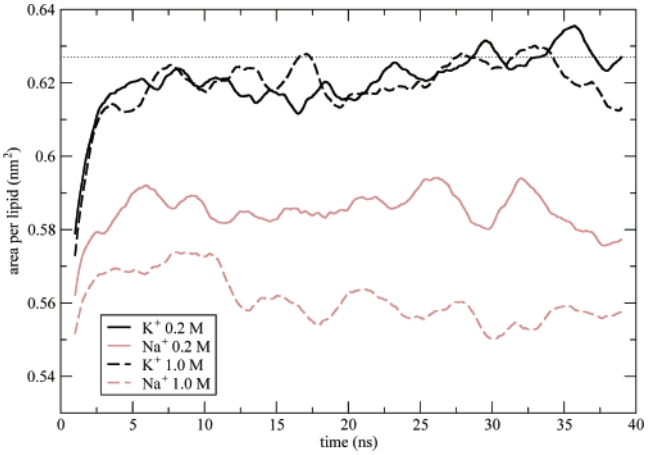

Figure 1. Time evolution of the area per lipid for the simulations with 0.2 M salt concentration and for the simulations with 0.2 and 1.0 M concentration of either NaCl or KCl. The curves are running averages over 2 ns. The straight dotted lines indicate the average area per lipid of the salt-free system.

KCl exhibit a differential behavior, showing no binding of potassium ions to the lipid head-group oxygens. A detailed analysis of these results is discussed below.

Figure 1 displays the time evolution of the area per lipid for the different simulations. The plot on the top displays the different systems with a 0.2 M saline concentration, whereas the one on the bottom shows a comparison of the simulations performed at 0.2 and 1 M concentration of sodium and potassium chlorides. As can be seen, in all cases the area per lipid reaches a plateau within 25 ns of simulation, indicating that the protocol used (see Methods) provided steady values for the areas much faster than usually required. The key point of the methodology used in the present work is to use a box of a DPPC bilayer and a 0.2 M NaCl aqueous solution generated using a cutoff to treat long-range interactions. In this conditions, ions,[18] similarly to special group charges, artificially enhance lipid order.[58] Figure 2 shows the time evolution of the average number of ions bound per lipid, showing that, with the exception of the LiCl system, this parameter reaches a steady state within 5 ns. In the case of LiCl, the much longer simulation time required is related to the special behavior of the system, in which virtually all ions are bound to the bilayer at the end of the trajectory. This figure also shows that in the case of 1 M NaCl, as well as in the two simulations of KCl, the number of ions bound to the membrane decrease with time. This supports that the procedure used is robust enough to release the excess ions produced when sodium cations are mutated to different ones (see Methods). In contrast, Figure 3 displays the time evolution of the average number of lipids per ion, indicating that the system is not completely equilibrated for some polyvalent ions. Indeed, the equilibration process requires lateral rearrangement of lipids which is a rather slow process[22] that has not yet converged in the present calculations. For this purpose, larger calculations are required that are beyond the scope of the present report.

Preferred Ionic Locations. Before discussing the effects of the ions upon the DPPC bilayer, we characterize the distribution of the important lipid head-group atoms. Plots of the number densities for the ions, phosphorus, and nitrogens are given in Figure 4 for systems with 0.2 M salt or no ions. The curves show average values over the two halves of the bilayer. In Table 2 we show positions of the maxima of the distributions and the distances between some of the maxima. The cations, except the potassium, are concentrated in a region 1.2−2.5 nm from the center of the bilayer. The center of the distribution is located between the carbonyl and the phosphate oxygens of the lipids. In contrast, the potassium ions do not show a maximum in their distribution, suggesting that they are not bound to the bilayer. A closer inspection of the profiles shows minor differences (less than 0.2 nm) between the positions of the maxima in the other cation distributions.

The chloride ions are in all systems spread over a much wider region than the cations. There is a maximum in the distribution (except for KCl) but this is located just below 3 nm from the bilayer center, about 1 nm outside the maximum in the cation distribution. For the divalent and trivalent cations, the peaks become larger and wider with increasing charge because of the larger number of chloride ions present in the simulations. It is interesting to note that the chloride distribution in the system with $MgCl_2$ exhibits a shoulder at 2.3 nm. At this distance, chloride ions are necessarily coordinated to the cations bound to the membrane, suggesting a strong association between magnesium and chloride ions. A similar behavior is observed for the system with $AcCl_3$. In the system with KCl, the chloride density in the region below 4 nm from the bilayer center is even lower because there is no cationic charge density to be neutralized. The degree of chloride penetration to the membrane decreases in the following order for the different cations: $Mg^{2+} > Ac^{3+} > Ca^{2+} \approx Sr^{2+} \approx Ba^{2+} > Li^{+} \approx Na^{+} > K^{+}$. Further, the compensation of cation charge results in a stronger association between chloride and cations when the charge of the latter increases. As shown in Table 2, the distance between the maxima in the cation and the chloride distributions varies between 0.7 and 1.2 nm and indicates an inverse correlation with the total charge bound to the lipid head-groups (see below).

Number of Bound Ions. The computed radial distribution functions (rdf) of the water oxygens relative to the cations were used to define ion binding. Ions closer than the cutoff distance in column four of Table 1 were considered as bound. The first peak of the rdf, which lies between 0.20 and 0.30 nm, depending on ion size, contains the first coordination shell; that is, these ions are considered as directly bound. The average number of cations bound per lipid computed during the last 15 ns of each simulation is shown in Table 3. All systems at 0.2 M salt concentration except KCl and LiCl contained 0.16−0.18 bound cations per lipid which corresponds to about 70% of the cations. At 1 M concentration, the corresponding numbers were 0.32 and 25%. To better understand these values, two simple estimates were performed considering the coordination properties of each ion type reported. First, a lower limit was obtained considering the average number of lipids per ion computed from the simulations and assuming that a lipid can only be part of the first or the second coordination shell of only one ion at a time. Similarly the maximum number of ions that a bilayer can bind can be determined by dividing the number of lipid oxygens in the system by the average number of lipid oxygens participating in both the first and the second coordination shell. In all cases, the actual values in the simulations are within, or close to, the limits obtained from these approximations.

In the simulations performed at 0.2 M salt concentration, the largest number of lipid bound cations was found for LiCl. Further, the number of bound ions decreases with increasing radius for the single charged (alkali) ions. Contrary to this, the number of bound divalent and trivalent ions is almost equal, independent of the radius. The simulations performed at 1 M salt concentration still show no potassium binding while the number of bound sodium ions almost doubles due to the fivefold increase of total ionic concentration. This suggests that the ion

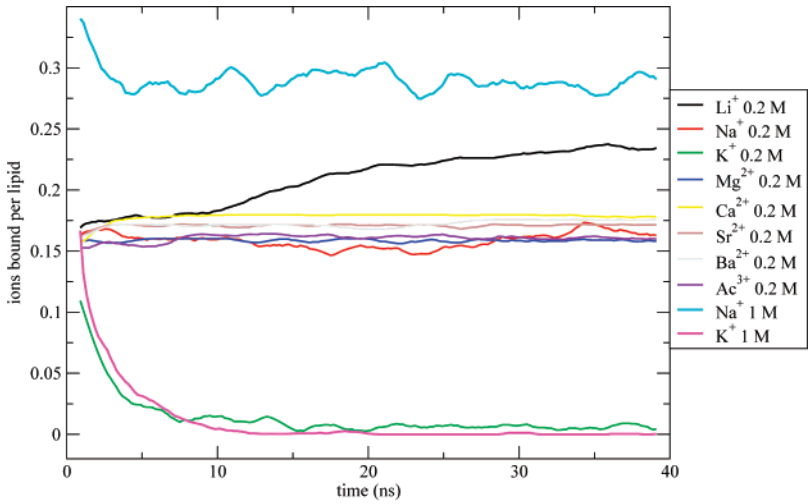

Figure 2. Time evolution of the number of ions per lipid bound to the lipid oxygen atoms.

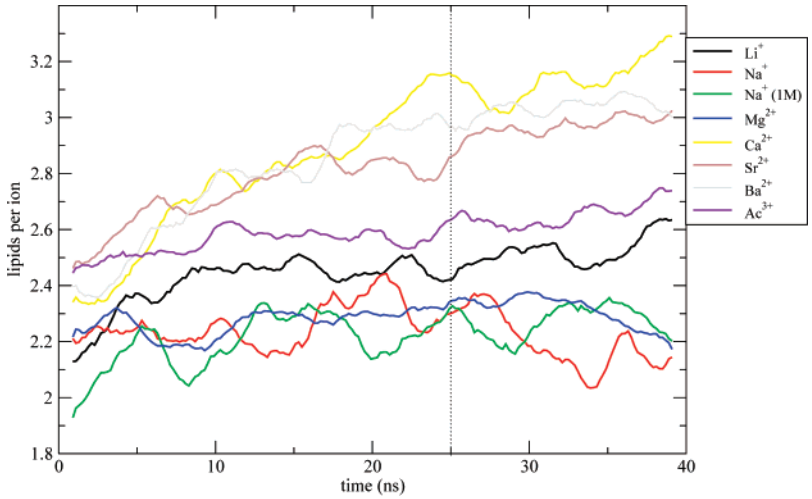

Figure 3. Time evolution of the number of lipids per ion.

binding is concentration dependent, although saturation can be achieved. As seen from Table 3, the maximum number of bound ions in the present simulations occurs with 1 M NaCl and is about one cation per three lipids. Even if we are starting to see saturation, it is still possible that this number could be slightly increased with salt concentrations beyond 1 M. The maximum bound positive charge per lipid is observed for 0.2 M $AcCl_3$ (about 0.5). Since we have not performed simulations with the divalent and trivalent ions at higher concentrations, we could not exclude that even more charge could bind to the membrane under such conditions. The present results also suggest that the bilayer might accommodate a larger number of lithium ions since they are smaller and bind in larger amounts to the bilayer at 0.2 M concentration. Moreover, it is also clear from the results for divalent and trivalent ions that the amount of charge provided by the monovalent ions is not limiting their binding.

Charge Distributions. The number density distributions of the phosphorus and the nitrogen atoms of the PC moiety are shown in Figure 4. The location of these atoms is crucial for the structure of the lipid bilayer. The distance between the peaks of these distributions directly reflect the tilt of the main part of the head-group dipole. A smaller contribution comes from the carbonyl dipoles. This affects directly the charge distribution perpendicular to the membrane surface and the dipole potential across the head-group region. The binding of cations in the lipid head-group region has a pronounced effect on the distribution of these groups. We observe that the maximum in the phosphorus density is shifted toward the water phase in the presence of all salts except KCl, in agreement with the increase in thickness (and decrease in the area per lipid) observed in previous simulations of PC lipids in sodium chloride.[18,21,22] In all cases, this shift is accompanied by a reduction of the peak width, meaning that not only the bilayer thickness increases but also the lipid head positions become more well defined. This is related to the increased order of the system. The densities of both nitrogens and ester carbonyl oxygens (not shown) exhibit similar profiles as that of the phosphorus atoms and are affected in a similar way by the presence of ions. It can be seen in Table 2 that the locations of the oxygen atoms relative to the phosphorus are maintained in all cases. However, the presence of ions results in sharper distributions with reduced tails toward the water phase. The choline nitrogen distributions (Figure 4) are, in the presence of salts other than KCl, shifted toward the water phase (up to 0.35 nm) with the peak width relatively unaltered. This shift and the associated change of the charge distribution are due to the repulsive interactions between the choline nitrogens and the cations as well as due to the attractive forces between the anions and the PC groups.

The computed charge distributions perpendicular to the bilayer surface are shown in Figure 5 for the salt-free system and the systems with 0.2 M salt. Each system should, on average, be symmetric about the center of the membrane. Further, the existence of boundary conditions means that there could not be an electrostatic potential difference across the

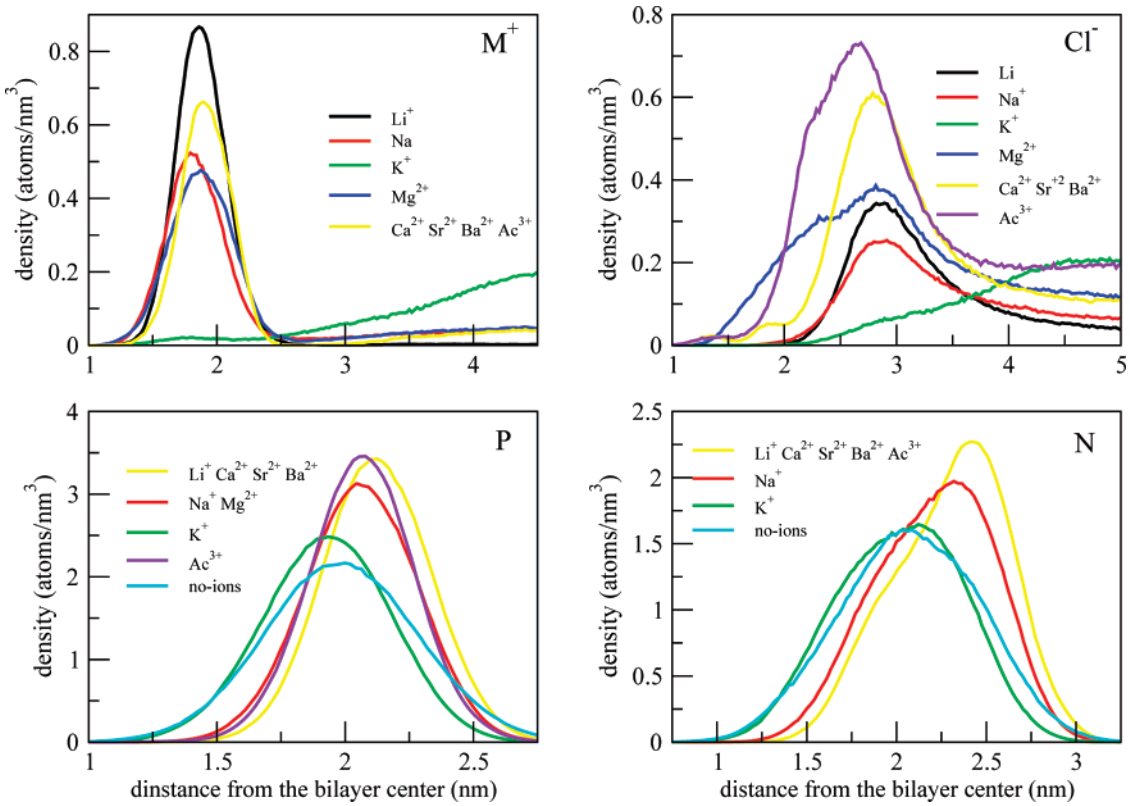

Figure 4. Partial number densities along the direction perpendicular to the bilayer plane for cations (top left), chloride ions (top right); the lipid phosphorus atoms (bottom left) and the nitrogen atoms (bottom right).

TABLE 2: The Position (nm) Relative to the Center of the Membrane of the Maxima in Different Number Density Profiles (left-hand side). The Distance (nm) between Some of the Peaks (right-hand side)[a]

	density distributions maxima						distances between maxima				
	P	N	OP	OC	M	Cl	P−N	OP−M	OC−M	P−Cl	Cl−M
no ions	2.00	2.08	2.02	1.61			0.08				
Li^+	2.12	2.41	2.12	1.72	1.86	2.89	0.29	0.26	0.14	0.77	1.03
Na^+	2.04	2.32	2.09	1.68	1.79	2.91	0.28	0.30	0.11	0.87	1.12
K^+	1.93	2.12	1.97	1.54			0.19				
Mg^{2+}	2.06	2.33	2.10	1.69	1.87	2.82	0.27	0.23	0.18	0.76	0.95
Ca^{2+}	2.11	2.43	2.12	1.73	1.89	2.79	0.32	0.23	0.16	0.68	0.90
Sr^{2+}	2.11	2.39	2.11	1.73	1.92	2.78	0.28	0.19	0.19	0.67	0.86
Ba^{2+}	2.12	2.40	2.12	1.73	1.90	2.74	0.28	0.22	0.17	0.62	0.84
Ac^{3+}	2.08	2.40	2.08	1.71	1.92	2.68	0.32	0.16	0.21	0.60	0.76

[a] P stands for phosphorous; N stands for nitrogen; OP stands for phosphate oxygens; OC stands for carbonyl oxygens; M stands for the different cations; and Cl for chloride ions.

periodic box. Therefore, the curves displayed are an average of both leaflets. The main feature of the charge distribution is consistent with the number densities of nitrogen and phosphorus atoms displayed in Figure 4. The charge distribution exhibits two regions with nonzero charge density: a negative one provided by the phosphate groups, and a positive one to the choline groups. Consequently, this charge distribution generates an electric dipole which is partially compensated by an opposing dipole generated by the polarized water molecules (see Figure 5). The result is a smooth total charge distribution, with maximum values about ± 0.1 charges/nm^3. Three different types of charge distribution profiles can be identified: (1) the profile of the bilayer and water without ions; (2) the system containing KCl; (3) the systems with the remaining salts studied. The main difference between these profiles lies in the presence of a peak at 2.5 nm which occurs in all systems except those without salt or with KCl, originating from the shift of the choline groups toward the water phase driven by the binding of cations to the bilayer. Both the salt-free system and that with KCl have single positive maxima close to the maximum of the phosphorus density distribution because in the latter, the potassium and the chloride ions are almost uniformly distributed. The systems with the remaining salts also exhibit differences in their charge density profiles since the location of the maxima in the charge distributions depends on charge and number of bound ions. The region with negative charge density is broader than that with positive charge, consistent with the broader distribution of chloride ions shown in Figure 4. Two major peaks with positive charge density are observed 2.0 and 2.5 nm from the bilayer center originating from the cations and choline nitrogens, respectively. In addition, a smaller maximum in the charge density can be observed at 1.3 nm originating from the ester carbons. This peak is not observed in the salt-free system, suggesting that the ions polarize the ester groups. On the other hand, minima in the charge density are found around 1.7, 2.2,

TABLE 3: Summary of the Computed System Properties

	ion/lipid						
	computed[a,b]	estimated minimum[b]	estimated maximum[c]	charge bound/lipid (e)[d]	dipole angle (deg)	area/lipid (nm^2)[e]	drop area lipid/ion lipid (nm^2)
no ions	0.00	–	–	0.097	14.7	0.627	–
Li^+ 0.2 M	0.23	0.17	0.28	0.184	28.5	0.557	0.300
Na^+ 0.2 M	0.17	0.18	0.28	0.161	23.8	0.585	0.247
Na^+ 1 M	0.32	0.18	0.28	0.186	28.0	0.556	0.222
K^+ 0.2 M	0.01	–	–	0.110	14.9	0.627	–
K^+ 1 M	0.00	–	–	0.109	16.0	0.623	–
Mg^{2+} 0.2 M	0.17	0.17	0.31	0.184	28.6	0.583	0.258
Ca^{2+} 0.2 M	0.18	0.14	0.21	0.208	33.0	0.548	0.440
Sr^{2+} 0.2 M	0.17	0.14	0.20	0.205	32.4	0.555	0.419
Ba^{2+} 0.2 M	0.18	0.14	0.20	0.206	32.2	0.557	0.399
Ac^{3+} 0.2 M	0.16	0.15	0.22	0.221	35.0	0.561	0.402

[a] Computed average number of ions bound per lipid. [b] See text. [c] Positive charge bound per lipid (including cations, chloride ions, and water). [d] Angle between the P−N vector and the bilayer plane. [e] Ration decrease area per lipid/ion per lipid.

and 2.5−3.0 nm due to the ester carbonyl oxygens, the phosphate oxygens, and the chloride ions, respectively.

As discussed above, the binding of ions to the lipid head-groups creates a charge dipole of cations and chloride ions which qualitatively resembles the charge dipole profile of polarized water molecules close to the bilayer head-groups. Interestingly, the magnitudes of the maxima in the charge densities provided by both the cations and the chloride ions are comparable or larger than those of the lipid head-groups in the system without ions. Furthermore, it is clear that the ionic charge densities alter the charge density distributions of lipid head-groups and water, resulting in a different net distribution. From the plots in Figure 5, the cumulative charge, including the net ionic charge and that of the polarized water, is obtained by integration over the spatial dimension perpendicular to the bilayer from the center out to the box limits. Since the system is neutral, this net charge will vanish at some distance which typically is about 3.5 nm from the center. Then, the total positive charge bound to the bilayer is taken from the maximum of the integrated charge density, typically about 2.25 nm. From the number of ions per lipid listed in Table 3, it can easily be seen that the charge bound per lipid at 0.2 M ranges between 0.10 and 0.22, where the

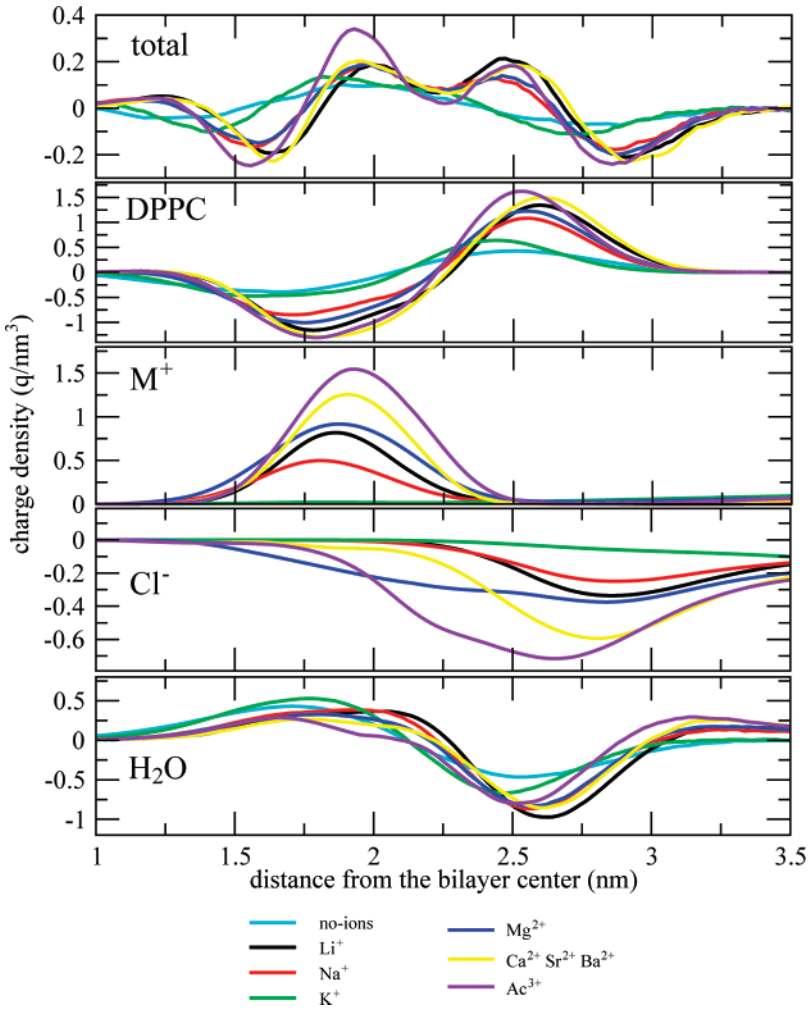

Figure 5. Charge densities in the direction perpendicular to the bilayer plane.

TABLE 4: Total Electrostatic Potential Difference (V) between the Center of the Water Layer and the Center of the Membrane, the Separate Contributions from Lipids, Ions, and Water, and an Approximate Result for the DPPC Head-Group Lipids[a]

ion	total	DPPC	ions	H_2O	DPPC (dipole approx)
no ions	−0.55	4.95	0.00	−5.48	2.60
Li^+ 0.2 M	−0.73	9.35	−11.60	1.51	5.69
Na^+ 0.2 M	−0.66	7.79	−7.37	−1.06	4.55
Na^+ 1 M	−0.66	9.14	−9.36	−0.87	5.63
K^+ 0.2 M	−0.54	5.02	−0.41	−5.13	2.63
K^+ 1 M	−0.51	4.96	−0.09	−5.48	2.85
Mg^{2+} 0.2 M	−0.73	9.06	−10.30	0.51	5.49
Ca^{2+} 0.2 M	−0.75	10.50	−13.13	1.83	6.70
Sr^{2+} 0.2 M	−0.71	10.15	−12.39	1.49	6.52
Ba^{2+} 0.2 M	−0.73	10.15	−12.55	1.65	6.40
Ac^{3+} 0.2 M	−0.69	10.32	−12.39	1.32	6.97

[a] The DPPC head-groups are represented by a positive electron charge and a negative electron charge located at each end of a vector of length 0.36 nm forming the angle with the membrane plane given in Table 3.

lowest values correspond to the system without salt or with KCl. Interestingly, these results suggest that the total bound charge does not increment much upon ion binding, indicating that there are other changes in the system that smooth the additional charge, specifically in the lipid bilayer, the chloride, and the water distributions.

The electrostatic potential was computed by integrating the one-dimensional Poisson equation twice:

$$\frac{\partial^2 \phi}{\partial z^2} = \frac{\rho(z)}{\epsilon_0} \tag{1}$$

where Φ is the electrostatic potential, the charge density $\rho(z)$ is taken from Figure 5, and ϵ_0 is the dielectric permittivity of vacuum. For boundary conditions, we put the potential and its derivative to zero in the center of bilayer. The resulting total potential is shown in Table 4 together with the individual contributions of each part of the system. Consistent with the results reported in previous simulations,[23,53] the total potential difference across the membrane/water interface in the system without ions is −0.55 V, resulting from a lipid contribution of +4.95 V and a water contribution of −5.48 V. The two simulations with KCl exhibit similar values, with a minor decrease in the system with the highest salt concentration. Further, it can be seen that the net potential difference from the potassium and chloride ions is small or negligible in these systems.

For the systems containing salts other than KCl, the total potential difference across the bilayer/water interface may be up to 50% larger than for the salt-free system. However, these net values are small compared to the potential difference created just by the ions, which ranges between 8 and 12 V in the present systems, because the lipid head-group and the water molecules shield it.[21] The ionic distribution corresponds to an electric dipole with its positive end oriented toward the membrane, whereas the dipole from the lipid head-groups is oppositely oriented. The results indicate that the ions induce a change in head-group tilt that increases the size of the lipid dipole, and of the potential, almost by a factor two. Additionally, the positive end of the net dipole from water, that pointed toward the membrane in the salt-free system, changes to the opposite direction with the presence of salt. Therefore, in addition to the 7.5−10.5 V potential from the lipid head-group, water provides about +1.5 V in the same direction which compensates most of the ionic potential.

Effects on the Lipid Head-Group. The cations bound to lipid head-group oxygens exert a repulsive force on the choline groups, pushing them further out into the water environment in agreement with early experimental results.[32] This observation is consistent with the role of lipid head-groups as charge sensors which was pointed out in early works[60,61] and in recent reports based on MD simulations. More precisely, a change in the orientation of the lipid head-groups can alleviate the charge provided by the bound ions.[18,19,21,22,48] The average lipid head-group dipole tilts obtained from the present calculations, measured from the bilayer plane, are reported in Table 3. The average angle of the dipole in a system without ions is 15°, in good agreement with other results of different PC bilayers, which ranged between 10 and 20°.[17−21]

Inspection of the table indicates that this angle may increase by up to 20° depending on ion type and salt concentration. The values obtained are in qualitative agreement with similar studies with bilayers with NaCl[20,21] and 0.2 M $CaCl_2$[22] despite that the results cannot be directly compared because of the different concentrations and waters/lipid and ions/lipid ratios. In the simulations with NaCl an increased dipole angle is observed with increasing salt concentration, consistent with the larger number of ions bound to the bilayer. In contrast, KCl results in a negligible effect on the dipole angle, which remains very close to that of the salt-free system both at 0.2 and 1 M salt concentration. The simulations indicate that in the present interval of bound charges (0−0.5 positive charges per lipid), the dipole angle with respect to the membrane plane increases with about 40° per positive charge and lipid.

The tilt angle correlates well with the bound ionic charge per lipid integrated from the sum of the charge distributions of the ions and the water molecules described in the preceding section (see Table 2). These results support the idea of lipid head-groups being charge sensors suggested in early experimental work. The electrostatic potential change across the lipid/water interface can be calculated by integrating the charge density from lipids, ions, and water twice in the Poisson equation. Using the charge neutrality of the system on may show that:

$$\Delta\phi = \frac{1}{\epsilon_0}\frac{P}{A}$$

where P/A is the total dipole moment per unit area, defined from the charge distribution or the positions of the individual charges as:

$$\frac{P}{A} = \int z\rho(z)\,\mathrm{d}z = \frac{1}{A}\sum_i q_i z_i$$

For the lipid part of this dipole, one has to include all the fractional charges of the lipids including the carbonyl dipoles and the actual charge distribution between phosphates, oxygen, nitrogen, and hydrocarbon groups. A common simplified model is to consider the head-group as consisting of one full negative charge at the position of the phosphorus and one full positive charge at the position of the nitrogen or still simpler as a full negative and positive charge at a distance of 0.36 nm. This corresponds to a dipole of 5.76×10^{-29} C m =17.3 debye. In such a model, the contribution to the electrostatic potential change across the lipid/water interface from the lipids is entirely

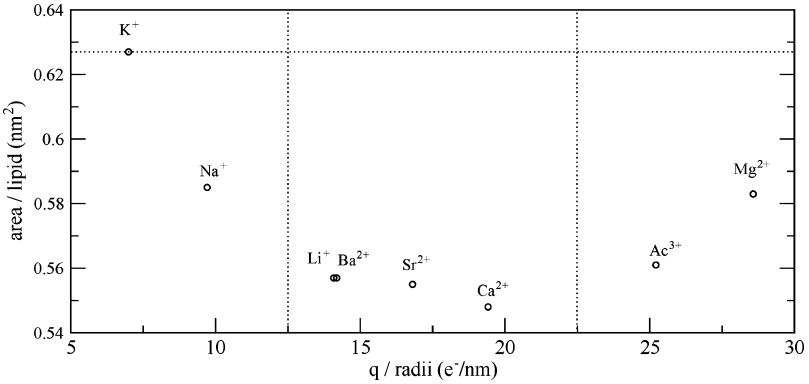

Figure 6. Area per lipid versus the ratio of charge/radii for the cations in the simulations at 0.2 M chloride salt concentration.

given by the tilt angle θ of this dipole and the area per lipid, *A*, as:

$$\Delta\phi = \frac{1}{\epsilon_0}\frac{P}{A}\sin\theta$$

The potential change in this dipole approximation has been calculated and is shown in the last column of Table 4. These values are smaller than those calculated from the full actual charge distribution, but there is a good correlation as $\Phi = 1.34\Phi_{dip} + 1.47$, indicating that the actual charge distribution has, in addition to this simplified model, contributions that increase the total dipole perpendicular to the bilayer with a constant value as with a dipole that is parallel to the PN dipole. The main contribution to this comes from the carbonyl region.

Ordering of the Lipid Molecules. The ordering in a lipid bilayer may be characterized by NMR order parameters, from fraction *trans* bonds, or from the area per lipid. All these measures are fairly well correlated. Although the area per lipid is not easily accessible experimentally, it is easy to calculate from simulations. Average values from the present simulations (shown in Table 3) provide clear evidence that the binding of cations to the lipid head-groups exerts an effect on the area per lipid. The bilayers exhibit in most cases smaller areas per lipid and larger thicknesses in agreement with previous results.[18,21] The latter can be easily monitored from the density distributions of the lipid phosphate moieties shown in Figure 4. In the system without salt each monolayer exhibits the maximum number density centered about 1.9 nm from the bilayer center, while the simulations with salts other than KCl have the maximum shifted toward the water environment on each monolayer. Moreover, the ions induce a narrowing of the distribution width, suggesting that the induced lipid order is associated with a less fluctuating distribution of the phosphate moiety relative to the bilayer center. In spite of the almost negligible number of ions bound to the PC moieties in the potassium-containing systems, density distribution exhibits an equally pronounced narrowing of the peak, which seems to be the reason for the small shift of the maximum toward the bilayer center.

The area per lipid for the salt-free DPPC bilayer is 0.627 ± 0.005 nm^2 in the present simulations, in good agreement with the experimental value of 0.64 ± 0.02 nm^2 reported for a pure fully hydrated DPPC bilayer in the liquid crystalline phase.[62] In contrast, the area per lipid computed from the simulations with salts other than KCl exhibit smaller values, as it is also reported in recent MD studies performed on Na^+-DPPC[18] and Na^+/Ca^{2+}-POPC[21,22] systems. Contrary to this, the area per lipid for the systems with both concentrations of KCl is similar to that of the salt-free system, which is consistent with our observation that potassium ions do not bind to the lipid head-groups and with recent experimental results for KBr.[42] Sodium exhibits a decrease in the average area per lipid, which gets slightly more pronounced at the highest concentration, similarly to the results reported in ref 21. The results for monovalent ions show a correlation between ordering effect, number of bound ions, and inverse ionic radii. For the same number of bound ions per lipid, the ordering effect upon the bilayer is larger for polyvalent than for monovalent ions.

Ion Features Contributing to the Area per Lipid. Present results indicate that each bound cation per lipid reduces the area per lipid, typically about 0.3 nm^2 (see Table 3), with differences depending on the ion type and with the largest effect observed for calcium. Moreover, the simulations at different concentrations of NaCl suggest that we are starting to see saturation of the number of bound ions as also reflected in the area per lipid. A fivefold increase in the ion concentration results in a doubling of the amount of bound ions, but the effect of this doubling of the amount of bound ions on the area is less than half the effect of the first ions. All cations studied, except potassium, bind to the lipid oxygens, modify the tilt of the lipid dipole, induce rearrangements around lipid head-groups, and affect the order of the acyl chains. Thus, it is reasonable to hypothesize that the ordering effect produced by a cation will depend on the number of ions bound to the lipid molecules and on specific cation features such as the radii charge, coordination number (CN), and energy of hydration.

The effect upon the area per lipid from binding of cations can be rationalized in terms of the charge/radius ratio as shown in Figure 6. The ionic radii were computed by subtracting the water oxygen radius (assumed to be constant) from the maximum of the radial distribution function (rdf) of the water oxygens around the ion, according to the procedure described in a previous work.[40] This approximation avoids the uncertainties in ionic radii when bound to the membrane since they depend on the CN they exhibit. A value of 0.137 nm for the water oxygen radius gives the best fitting to the experimental radii[63] based on the actual CN for the ions when bound to the lipids obtained from the present calculations (see Table 1).

The plot of the area per lipid versus the charge/radius can be divided into three parts: First, monovalent ions with ratios between 0 and 14 exhibit a drop on the area from the value of the pure system up to the maximum decrease observed. Second, for divalent ions with ratios between 14 and 20 the drop is much smaller. Finally, for Mg^{2+} and Ac^{3+} ions, with ratios larger than 25, the behavior of the area per lipid changes and starts increasing again. There are different sources for this behavior as discussed below.

The strength of the interactions between the ions and the bilayer are of importance in order to explain the effects of ions

on lipid order. Recently, it has been shown that changes on the phase transition temperature of PC bilayers exhibit a linear correlation with the electrostatic free energy of the ions in water.[40] Thus, one would expect that the present results can be understood from the differences in ion/oxygen interaction potentials. In the present work the interaction between a cation and a water/lipid oxygen atom is the combined effect of the Coulombic and the Lennard−Jones (LJ) terms. These combine into a potential well that may be described by a depth and the position of the minimum. Since the Coulombic term is attractive and the LJ repulsive at shorter distances, for the same valence a cation with a larger radius exhibits a shallow minimum in the potential curve. The present results suggest that the K^+ well is so shallow that ions do not bind to the lipid head-groups. Despite the different ion force-fields available, the minimum has a similar energy in the commonly used force-fields (data not shown). Additionally, to the present simulation using the OPLS-AA force-field for ions, very recent results have shown a similar effect using GROMACS and CHARMM.[44] Moreover, the results shown in Figure 6 can be used as a predictive tool for other ions not present in this study. It is reasonable to expect that monovalent ions that are larger than potassium, e.g., rubidium and cesium, behave similarly, not binding to the lipid head-groups. Because of its shallow well, sodium exhibits the largest fluctuations in the number of ions bound (see Figure 2), suggesting that mean lifetime for a sodium−lipid complex is shorter than for other cations. In contrast, polyvalent ions exhibit a deeper well even for the largest ions studied since the larger Coulombic term compensates for the penalty on the well depth because of the radius.

A larger cation radius provides larger CN and therefore an additional number of binding possibilities to the lipid oxygens. Therefore, the computation of the CN for each ion type is necessary to understand the present results. The CN for the first shell were computed for cations coordinated either only to water oxygens or to the lipid oxygens in any extent. The cutoffs considered were taken from the positions where the first peaks in the rdf vanish (see Table 1). Additionally, the CN for the second shells were computed from the second peak in the rdf, which provides a cutoff approximately 0.25 nm larger than the first shell. According to the present simulations, the average CN for the first shell for the cations bound to at least one lipid atom range between 4 and 9, as shown in Table 5A. The average values are similar to those obtained in pure water and are in reasonable agreement with those recently reported in the literature for metal hydrates obtained either from experiments or *ab initio* calculations (see ref 64 and references therein). The magnesium ion is the only ion exhibiting a significantly different coordination than experimentally determined. However, a strong association with chloride, reflected in a large peak at 2.5 nm in the pair correlation function with the chloride ions, is observed (not shown) and may explain this behavior. A similar peak is observed at 3.0 nm for the lithium ion, but the larger distance seems to be the reason for the minor effect on the CN.

The CNs observed in the simulations for a specific ion may differ, as seen from the relative populations displayed in Figure 7a. For the cations with the same valence, a larger radius produces a shift of the most populated CN toward larger values, in agreement with experimental evidence and recent MD simulations.[22] The relatively wide distribution for potassium reflects the lower binding energy exhibited by this cation. Ions bound to the lipid head-groups are not completely surrounded by lipid oxygens and remain partially hydrated. Therefore, it may be better to use the actual number of lipid oxygens

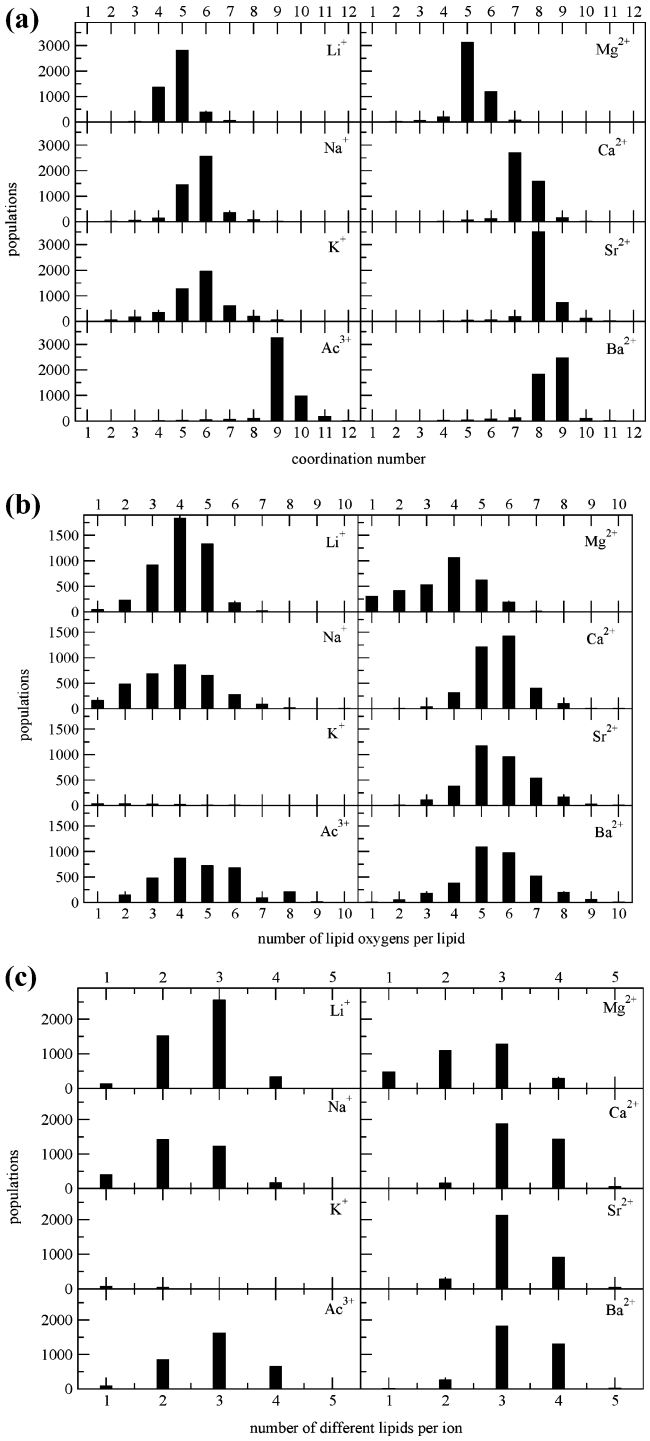

Figure 7. Populations for (a) the CN of the ions when bound to one or more lipid oxygen atoms. The coordinating atoms include water and lipid oxygens and chloride ions. (b) The number of lipid oxygens per cation. (c) The number of different lipids per cation.

coordinated to an ion instead of using the CNs given previously. Present simulations indicate that all cations, except potassium, have 3−5 lipid oxygens in the first coordination shell and 8−13 in the second (Table 5A), resulting in 11−18 lipid oxygens per cation in total. Each ion exhibits, however, a wide range of possible coordinations as can be seen from the populations displayed in Figure 7b.

These results suggest that ions can modulate lipid order by acting as cement between the neighboring lipids. If this is true, the modulation should depend on the number of different lipids

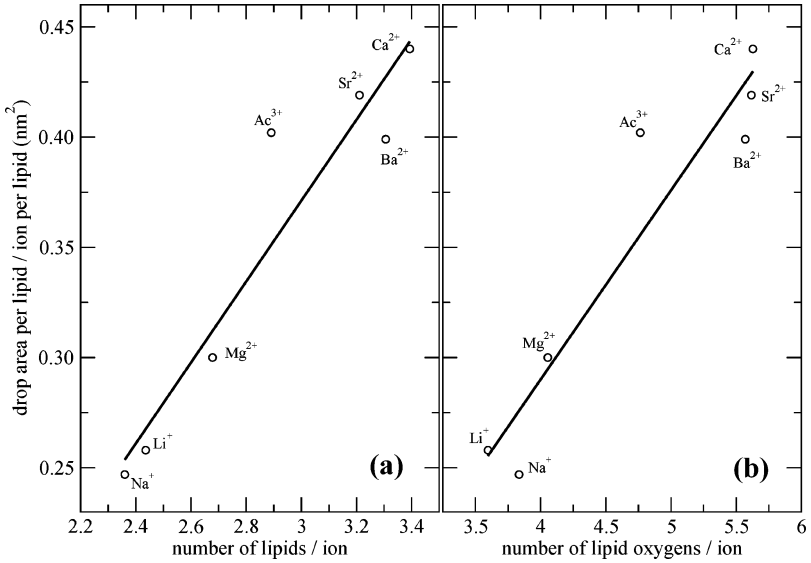

Figure 8. Drop in the area per lipid/ion per lipid ratio versus (a) the average number of different lipids bound per ion and (b) the average number of oxygens per ion, in the first coordination shell.

TABLE 5: Coordination Properties of Each Atom Type

A.

	coordination no. (CN)[a]			no. of lipid oxygens[b]			no. of lipids[c]		
ion	water	DPPC	water exp[d]	LipO^{1st}	LipO^{2nd}	Lip O^{tot}	1st CS	2nd CS	total
Li^+	4.7	4.8	4−5	4.1	10.3	14.3	2.7	3.1	5.8
Na^+	5.2	5.8	4−6	3.8	10.4	14.1	2.4	3.3	5.6
Na+ (1 M)	5.8	5.8	4−6	3.5	9.6	13.1	2.3	3.1	5.4
K^+	5.6	5.5	4−6	−	−	−	−	−	−
Mg^{2+}	4.8	5.4	6	3.6	9.2	12.8	2.4	3.4	5.8
Ca^{2+}	7.7	7.2	6−8	5.6	13.8	19.4	3.4	3.8	7.2
Sr^{2+}	8.0	8.2	7−8	5.6	14.5	20.2	3.2	3.8	7.0
Ba^{2+}	8.4	8.5	7−9.5	5.6	14.5	20.1	3.3	4.0	7.3
Ac^{3+}	9.0	9.2	−	4.8	13.2	17.9	2.9	3.9	6.8

B.

	no. of oxygens in the first coordination shell[f]				no. of oxygens in the second coordination shell[f]			
ion[e]	free PO_4^{2-}	ester PO_4^{2-}	free COO-R	ester COO-R	free PO_4^{2-}	ester PO_4^{2-}	free COO-R	ester COO-R
Li^+	1.9	0.1	1.9	0.1	4.1	4.2	2.8	3.2
Na^+	1.4	0.2	1.9	0.1	3.8	3.5	3.3	3.4
Na+ (1 M)	1.4	0.2	1.8	0.1	3.7	3.4	2.9	3.0
Mg^{2+}	1.6	0.1	1.9	0.0	4.1	3.4	2.8	2.2
Ca^{2+}	3.0	0.0	2.5	0.1	6.3	6.2	3.4	3.5
Sr^{2+}	2.9	0.1	2.5	0.1	6.2	6.0	3.9	4.1
Ba^{2+}	2.8	0.1	2.6	0.0	6.3	6.0	4.0	3.8
Ac^{3+}	2.6	0.1	2.0	0.0	6.2	5.5	3.5	2.8

[a] CN−exp represents the experimental CN in metal hydrates. [b] LipO^{1st}, LipO^{2nd}, and Lip O^{tot} refer to the average number of lipid oxygens present in the first, second, or both coordination shells, respectively. [c] Number of different lipids per cation in the first and second coordination spheres. [d] From Tables 4 and 6 of ref 64. [e] K^+ has not been included since the values are not meaningful due to the small number of ions bound to the bilayer. [f] CN−bound and −free indicate if the CN has been calculated for ions bound or free, respectively, to the lipid oxygens.

linked by a single ion. Therefore, an analysis of the average number of lipids per cation in the present trajectories has been performed. The results indicate that on average each ion interacts with 5.6−7.4 lipids of which 2.4−3.4 are in the first and 3.1−4.0 the second coordination shell. This indicates that despite differences in the average CN, the number of lipids that a cation can link increases only slightly for ions with larger CN. However, the results in Figure 3 suggest that longer simulations may provide slightly larger oxygens per ion for some polyvalent ions, as this parameter is not fully converged in 40 ns. Indeed, a recent MD study of the binding of Ca^{2+} ions to POPC bilayers observed about 4 lipids per ion.[22] However, although it is true that longer simulations would provide slightly larger values than reported in Table 5 A, they would still be smaller than 4 lipids as reported in the preceding reference. One possibility is that such differences arise from the force-field used for the ions, although it is also possible that they are due to the fact that the ratio ions/lipid is almost eight times larger in the present work, and therefore there are less free lipids. The histogram of the number of lipids per ion shown in Figure 7c reflects the wide range of possibilities. Moreover, ions exhibiting low CN require less lipid oxygens, and therefore the maximum number of ions that the bilayer can bind is larger.

The relative preference of the different cations for each of the four oxygen types present in a PC lipid is shown in Table 5B. This shows that the first coordination shell involves mainly

free (nonesterified) oxygens, either from the carbonyl or phosphate groups. The number densities shown in Figure 4 reveal that the cations are located in an intermediate region between the carbonyl and the phosphate oxygens. Table 5B shows that, in general, there is little difference in ion preference for different coordinating oxygens. The situation differs, however, if we look at each cation separately. Lithium interacts equally with both oxygen types, sodium and magnesium prefer the phosphate oxygens, and calcium, strontium, barium, and actinium prefer the carbonyl oxygens. Similar results are obtained from the rdf between cations and oxygen atoms (not shown). Regarding the second coordination shell, the present results suggest that the non-free oxygens are important as anchoring points for the water molecules that are part of the first coordination shell, specifically the esterified phosphate oxygens.

A recent study outlined the existence of discrepancies regarding the localization of cations within simulations.[19] Ion penetration must be sensitive to the strength of the interactions between hydrocarbon lipid tails and to the balance between LJ and electrostatic interactions in the different force-fields used. To our knowledge, there are three lipid force-fields that have been used in studies of cation−lipid interactions, the one implemented in CHARMM,[65] the one developed by Berger et. al[4] for GROMACS,[45,46] and the one designed by Smondyrev et. al[7] for AMBER.[66] In the present work we have used the parameters of Berger et al. in the context of the OPLS-AA implementation in GROMACS (see Methods), a widely used combination in membrane protein simulations.[67] With the lack of experimental information about the cation localization, none of these force-fields can *a priori* be considered better than the other for the present purposes. When more experimental information about specific binding of cations to lipid bilayers becomes available, it will be important to validate the different force-fields against that information, including ion parameters.[56]

The analysis performed above suggests that the coordination properties have effects, though small, on the reduction of the area per lipid per binding ion. The decrease in area per lipid (see Table 4) shows a reasonable linear correlation with the average number of lipid oxygens being part of the first coordination sphere of a cation (Figure 8a). A similar tendency is observed for the average number of lipid molecules linked by the same cation (Figure 8b). These results are of considerable importance since some of the ions included in this study, e.g., K^+, Na^+, Ca^{2+}, and Mg^{2+}, are abundant in the aqueous solution surrounding biological membranes.

Conclusions

The effect of including different chloride salts in the water surrounding a DPPC bilayer has been studied in the present work by means of MD simulations. For this purpose, 40 ns simulations of DPPC bilayers in 0.2 M chloride salts with the cations Li^+, Na^+, K^+, Mg^{2+}, Ca^{2+}, Sr^{2+}, Ba^{2+}, and Ac^{3+} were performed and analyzed. For sodium and potassium chlorides, additional simulations at a 1.0 M concentration allowed checking for concentration effects. A simulation without salt was also included and used as reference.

It is known that simulations of this kind of system require long sampling equilibration times. In order to reduce these times, the present calculations were carried out using a biased starting box generated using a treatment of the electrostatics that exaggerates lipid order and reduces area per lipid (see Methods). Since the presence of ions also favors small areas, the required times to obtain a steady state for the area per lipid, once the system is lifted from these conditions, is reduced. These results suggest that the procedure is robust enough to provide reliable simulations; however, the equilibration times are still larger since reaching a steady value for the area per lipid does not guarantee that lipid molecules have completed the process of adaptation around the cations.

The simulations indicate that most ions actually do bind to the lipid head-groups, being distributed in the lipid−water interface generating a double layer, organized in such a way that the positive ions sit closer to the bilayer interface. Potassium chloride is one exception that exhibits a differential behavior not showing any binding to the lipid head-groups. All the systems at 0.2 M salt concentration contained 0.16−0.18 bound cations per lipid except the systems with KCl and LiCl. Moreover, for the alkaline cations, this number decreases with size, whereas for the rest of the ions, the number is almost identical. For the system containing 1 M NaCl, only a moderate increase of the number of bound cations from 0.17 up to 0.32 is observed, suggesting that there is a limit for the number of cations, or cation charges, that each lipid can bind.

The charge density profile of the system has contributions from lipid head-groups, ions, and water. Each contribution gives rise to a change of the electrostatic potential across the membrane/water interface. The different contributions tend to compensate for each other and result only in a small net potential drop when passing from the membrane to the water. This is, however, increased from about 0.5 V to about 1 V in the presence of ions. The lipid dipoles point toward the water and would give rise to an increased electrostatic potential of the order of 5 V without the water. Without ions, the water will overshield the head-groups and result in a net potential change of −0.5 V. The ionic distribution contributes with a potential change of about −10 V, but because of a larger tilt of the head-groups the contribution from the lipids will double and cancel this almost totally. Additionally, the water polarization will change sign and be reduced considerably compared to that in the salt-free system, resulting in a net potential change of about −1 V. The maximum contribution observed from the lipid heads is about +10 V, suggesting that there is a limit for this value given by a maximum value at which the head-group dipoles may tilt out of the membrane plane. This could then determine the maximum number of possible bound ions that would not give rise to excessive electrostatic fields.

With the exception of potassium, present simulations show that a large fraction of the cations are located around the carbonyl and phosphate oxygens of the lipid head-groups, whereas the chloride ions are located further out in the aqueous phase. The distance between the maxima observed in the cations and the chloride ions density distributions range between 0.7 and 1.2 nm for the different systems. Therefore, the ion distribution generates a dipole moment that opposes the dipole moment of the lipid head-groups modulated by the one created by the polarized water molecules in the opposite direction. However, the results reported in the present work regarding cation distributions need to be validated when more experimental information about specific binding of cations to lipid bilayers becomes available. Until then, it will be difficult to evaluate the strengths and weaknesses of the different force-fields including lipids, ions, and water molecules as well as the lack of computing the electronic polarizability in the currently available lipid force-fields. As recently stated,[19] there are indeed

differences in the localization of cations between simulations using different force-fields[19,21−23] that are waiting to be clarified.

The most important result of the present work is the observation of large differences between different ions depending on size and charge. Ion binding produces more ordered bilayers, i.e., thicker bilayers, and consequently smaller areas per lipid. However, to obtain good qualitative results, it is necessary to run very long simulations especially for the ions with higher valence. The results are sensitive to the force-field as shown in ref 44, and further investigation of the possible artifacts produced is necessary.

The present results have remarkable interest because many of the ions studied, specifically K^+, Na^+, Ca^{2+}, and Mg^{2+}, are present in biological membranes. Moreover, given that membranes are the natural barriers between electrolyte solutions with different concentrations, the results provide evidence that the ionic environment provides a contribution that may drive membrane asymmetry. We expect that the present results can shed light on the experimental results published in the literature regarding the differential behavior of alkaline ions in membranes.

Acknowledgment. A.C. wishes to express his gratitude to the Technical University of Catalonia for a fellowship to undertake his doctoral studies. The Spanish Ministry of Science and Technology supported this work through grant number SAF2005-08148-C04-01

References and Notes

(1) White, S. H.; Wimley, W. C. *Annu. Rev. Biophys. Biomol. Struct.* **1999**, *28*, 319.
(2) Singer, S. J.; Nicolson, G. L. *Science* **1972**, *175*, 720.
(3) van der Ploeg, P.; Berendsen, H. J. C. *J. Chem. Phys.* **1982**, *76*, 3271.
(4) Berger, O.; Edholm, O.; Jähnig, F. *Biophys. J.* **1997**, *72*, 2002.
(5) Feller, S. E. *Curr. Opin. Colloid Interface Sci.* **2000**, *5*, 217.
(6) Tieleman, D. P.; Marrink, S. J.; Berendsen, H. J. C. *Biochim. Biophys. Acta* **1997**, *1331*, 235.
(7) Smondyrev, A. M.; Berkowitz, M. L. *J. Comput. Chem.* **1999**, *20*, 531.
(8) Lindahl, E.; Edholm, O. *Biophys. J.* **2000**, *79*, 426.
(9) Feller, S. E.; Gawrisch, K.; MacKerell, A. D., Jr. *J. Am. Chem. Soc.* **2002**, *124*, 318.
(10) Leekumjorn, S.; Sum, A. K. *Biophys. J.* **2006**, *90*, 3951.
(11) Gurtovenko, A. A.; Patra, M.; Karttunen, M.; Vattulainen, I. *Biophys. J.* **2004**, *86*, 3461.
(12) Pandit, S. A.; Bostick, D.; Berkowitz, M. L. *Biophys. J.* **2003**, *85*, 3120.
(13) Hofsäβ, C.; Lindahl, E.; Edholm, O. *Biophys. J.* **2003**, *84*, 2192.
(14) Pitman, M. C.; Suits, F.; Mackerell, A. D., Jr.; Feller, S. E. *Biochemistry* **2004**, *43*, 15318.
(15) Pitman, M. C.; Grossfield, A.; Suits, F.; Feller, S. E. *J. Am. Chem. Soc.* **2005**, *127*, 4576.
(16) Mukhopadhyay, P.; Monticelli, L.; Tieleman, D. P. *Biophys. J.* **2004**, *86*, 1601.
(17) Pandit, S. A.; Berkowitz, M. L. *Biophys. J.* **2002**, *82*, 1818.
(18) Pandit, S. A.; Bostick, D.; Berkowitz, M. L. *Biophys. J.* **2003**, *84*, 3743.
(19) Sachs, J. N.; Nanda, H.; Petrache, H. I.; Woolf, T. B. *Biophys. J.* **2004**, *86*, 3772.
(20) Gurtovenko, A. A. *J. Chem. Phys.* **2005**, *122*.
(21) Böckmann, R. A.; Hac, A.; Heimburg, T.; Grubmüller, H. *Biophys. J.* **2003**, *85*, 1647.
(22) Böckmann, R. A.; Grubmüller, H. *Angew. Chem., Int. Ed.* **2004**, *43*, 1021.
(23) Berkowitz, M. L.; Bostick, D. L.; Pandit, S. *Chem. Rev.* **2006**, *106*, 1527.
(24) Parsegian, V. A. *Ann. N. Y. Acad. Sci.* **1975**, *264*, 161.
(25) Loosleymillman, M. E.; Rand, R. P.; Parsegian, V. A. *Biophys. J.* **1982**, *40*, 221.
(26) Tatulian, S. A. *Eur. J. Biochem.* **1987**, *170*, 413.
(27) Cunningham, B. A.; Gelerinter, E.; Lis, L. J. *Chem. Phys. Lipids* **1988**, *46*, 205.
(28) Roux, M.; Bloom, M. *Biochemistry* **1990**, *29*, 7077.
(29) Clarke, R. J.; Lupfert, C. *Biophys. J.* **1999**, *76*, 2614.
(30) Akutsu, H.; Seelig, J. *Biochemistry* **1981**, *20*, 7366.
(31) Altenbach, C.; Seelig, J. *Biochemistry* **1984**, *23*, 3913.
(32) Brown, M. F.; Seelig, J. *Nature* **1977**, *269*, 721.
(33) Lis, L. J.; Lis, W. T.; Parsegian, V. A.; Rand, R. P. *Biochemistry* **1981**, *20*, 1771.
(34) Lis, L. J.; Parsegian, V. A.; Rand, R. P. *Biochemistry* **1981**, *20*, 1761.
(35) Herbette, L.; Napolitano, C. A.; McDaniel, R. V. *Biophys. J.* **1984**, *46*, 677.
(36) Elmore, D. E. *FEBS Lett.* **2006**, *580*, 144.
(37) Zhao, W.; Rog, T.; Gurtovenko, A. A.; Vattulainen, I.; Karttunen, M. *Biophys. J.* **2007**, *92*, 1114.
(38) Watts, A.; Harlos, K.; Marsh, D. *Biochim. Biophys. Acta* **1981**, *645*, 91.
(39) Hauser, H.; Shipley, G. G. *Biochemistry* **1984**, *23*, 34.
(40) Binder, H.; Zschornig, O. *Chem. Phys. Lipids* **2002**, *115*, 39.
(41) Garcia-Manyes, S.; Oncins, G.; Sanz, F. *Biophys. J.* **2005**, *89*, 1812.
(42) Petrache, H. I.; Tristram-Nagle, S.; Harries, D.; Kucerka, N.; Nagle, J. F.; Parsegian, V. A. *J. Lipid Res.* **2006**, *47*, 302.
(43) Pedersen, U. R.; Leidy, C.; Westh, P.; Peters, G. H. *Biochim. Biophys. Acta* **2006**, *1758*, 573.
(44) Gurtovenko, A. A.; Vattulainen, I. *Biophys. J.* **2007**, *92*, 1878.
(45) Berendsen, H. J. C.; van der Spoel, D.; van Drunen, R. *Comput. Phys. Commun.* **1995**, *91*, 43.
(46) Lindahl, E.; Hess, B.; van der Spoel, D. *J. Mol. Model.* **2001**, *7*, 306.
(47) Berendsen, H. J. C.; Postma, J. P. M.; DiNola, A.; Haak, J. R. *J. Chem. Phys.* **1984**, *81*, 3684.
(48) Gambu, I.; Roux, B. *J. Phys. Chem. B* **1997**, *101*, 6066.
(49) Tieleman, D. P.; Berendsen, H. J. C. *J. Chem. Phys.* **1996**, *105*, 4871.
(50) Miyamoto, S.; Kollman, P. A. *J. Comput. Chem.* **1992**, *13*, 952.
(51) Darden, T.; York, D.; Pedersen, L. *J. Chem. Phys.* **1993**, *98*, 10089.
(52) Cordomi, A.; Edholm, O.; Perez, J. J. *J. Comput. Chem.* **2007**, *28*, 1017.
(53) Wohlert, J.; Edholm, O. *Biophys. J.* **2004**, *87*, 2433.
(54) Jorgensen, W. L.; Maxwell, D. S.; TiradoRives, J. *J. Am. Chem. Soc.* **1996**, *118*, 11225.
(55) Jorgensen, W. L.; Chandrasekhar, J.; Madura, J. D.; Impey, R. W.; Klein, M. L. *J. Chem. Phys.* **1983**, *79*, 926.
(56) Patra, M.; Karttunen, M. *J. Comput. Chem.* **2004**, *25*, 678.
(57) Patra, M.; Karttunen, M.; Hyvonen, M. T.; Falck, E.; Vattulainen, I. *J. Phys. Chem. B* **2004**, *108*, 4485.
(58) Patra, M.; Karttunen, M.; Hyvönen, M. T.; Falck, E.; Lindqvist, P.; Vattulainen, I. *Biophys. J.* **2003**, *84*, 3636.
(59) Cordomi, A.; Perez, J. J. *J. Phys. Chem.* B. **2007**, *111*, 7052.
(60) Seelig, J.; Macdonald, P. M.; Scherer, P. G. *Biochemistry.* **1987**, *26*, 7535.
(61) Akutsu, H.; Nagamori, T. *Biochemistry.* **1991**, *30*, 4510.
(62) Nagle, J. F.; Tristram-Nagle, S. *Biochim. Biophys. Acta* **2000**, *1469*, 159.
(63) Shannon, R. D. *Acta. Crystallogr.Sect. A: Found. Crystallogr.* **1976**, *32*, 751.
(64) Tunell, I.; Lim, C. *Inorg. Chem.* **2006**, *45*, 4811.
(65) Brooks, B. R.; Bruccoleri, R. E.; Olafson, B. D.; States, D. J.; Swaminathan, S.; Karplus, M. *J. Comput. Chem.* **1983**, *4*, 187.
(66) Pearlman, D. A.; Case, D. A.; Caldwell, J. W.; Ross, W. S.; Cheatham, T. E.; Debolt, S.; Ferguson, D.; Seibel, G.; Kollman, P. *Comput. Phys. Commun.* **1995**, *91*, 1.
(67) Tieleman, D. P.; MacCallum, J. L.; Ash, W. L.; Kandt, C.; Xu, Z. T.; Monticelli, L. *J. Phys. Condens. Matter* **2006**, *18*, S1221.